THE JOURNAL OF PHYSICAL CHEMISTRY Letters

pubs.acs.org/JPCL Letter

Experimental Observation of the Autler–Townes Splitting in Polyatomic Molecules

Junggil Kim, Jean Sun Lim, Heung-Ryoul Noh,* and Sang Kyu Kim*

Cite This: J. Phys. Chem. Lett. 2020, 11, 6791–6795

Read Online

ACCESS | Metrics & More | Article Recommendations | Supporting Information

ABSTRACT: Autler–Townes (AT) splitting has been experimentally observed in the optical transition between the zero-point levels of S_1 and S_0 for supersonically cooled 2-methoxythiophenol, 2-fluorothiophenol, and 2-chlorothiophenol. This is the first experimental observation of the light-dressed quantum states of polyatomic molecules ($N > 3$) in the electronic transition. In the resonance-enhanced ionization process involving the optically coupled states, if Rabi cycling is ensured within the nanosecond laser pulse, AT splitting is clearly observed for the open system for which the excited-state lifetime is shorter than hundreds of picoseconds. Semiclassical optical Bloch equations and a dressed-atom approach based on the three-level atomic model describe the experiment quite well, giving deep insights into the light–matter interaction in polyatomic molecular systems.

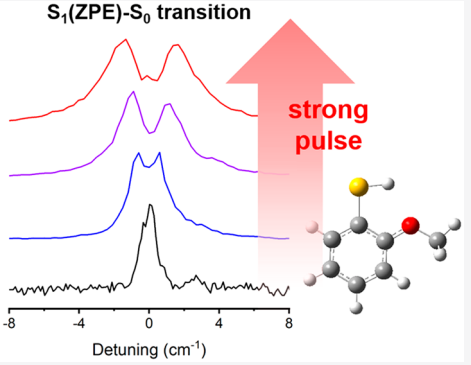

Autler–Townes (AT) splitting was discovered in 1955 for a microwave transition of the OCS molecule.[1] The AT doublet, caused by the strong resonant field between the optically coupled states, has since been generally accepted as the prototypical manifestation of the dynamic AC Stark effect. The dressed-atom approach that deals with the coupled system of atom and driving photons has been quite successful in explaining the experimental observation, providing the underlying physical insights. Actually, dressing the quantum state with the strong optical field is essential for the manipulation of atomic or molecular motions in terms of cooling,[2,3] trapping,[4] or controlling chemical reactions.[5−7] Although the AT splitting is quite general, its experimental observation has been mostly confined to atoms,[8−12] artificial atoms,[13−15] or diatomic molecules.[16−29] For instance, AT splitting has never been reported for polyatomic molecular systems ($N > 3$) in the electronic transition. In fact, AT splitting has not been anticipated for polyatomic molecules as obviously there are so many internal degrees of freedom that hamper the coherent Rabi oscillation. The high density of states in polyatomic molecules is strongly responsible for the lack of optical coherence. Therefore, it has long been well known that AT splitting should be negligible in the spectroscopy of polyatomic molecules.[30−35]

Surprisingly, however, AT splitting has been clearly observed here for polyatomic molecular systems under certain circumstances, allowing the direct observation of the dressed state in polyatomic molecules. The experiment could be explained well by the semiclassical optical Bloch equations based on the open three-state atomic model (Figure 1). Remarkably, AT splitting is found to be robust if the coherent Rabi frequency and dephasing dynamics of the coupled eigenstates are within certain ranges even for polyatomic molecules. As the AT splitting is a consequence of the light–molecule interaction, our new observation should shed new light on the manipulation of polyatomic molecules in terms of not only cooling or trapping but also control of the reaction.

Figure 1a shows the resonant two-photon ionization (R2PI) spectrum of supersonically cooled 2-methoxythiophenol (2-MTP; C_7H_8OS) which is a 17-atom molecule. The laser pulse with a temporal duration of 5 ns and a bandwidth of 0.4 cm^{-1} was used to pump the S_1 ($\pi\pi^*$)–S_0 transition of 2-MTP, whereas the D_0–S_1 ionization occurs within the same laser pulse. The R2PI spectrum then represents a variety of S_1–S_0 vibronic transitions, and the peak shape of each vibronic band reflects the rotational-state distributions of coupled states subject to symmetry conservation and rotational temperature. Under these supersonic jet conditions, the rotational temperature is estimated to be 1.1 K, and the peak shape of each vibronic band is supposed to be reproduced well by the simulation based on the asymmetric rotor analysis.[36] This method has been routinely applied for the spectral analysis of the R2PI bands in general. The influence of the increase in laser intensity is usually anticipated to be like the increase in peak intensity, saturation broadening, or the emergence of the

Received: June 20, 2020
Accepted: July 29, 2020
Published: July 29, 2020

https://dx.doi.org/10.1021/acs.jpclett.0c01918
J. Phys. Chem. Lett. 2020, 11, 6791–6795

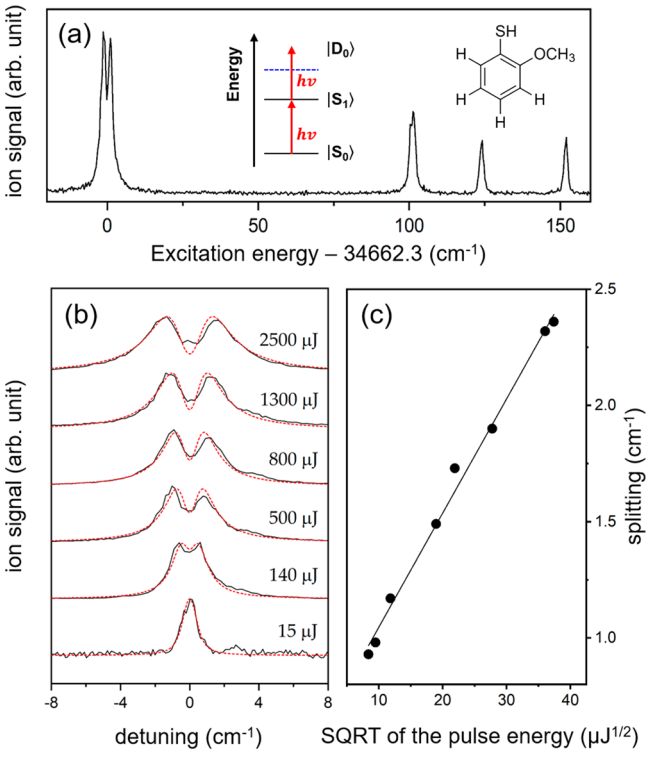

Figure 1. (a) R2PI spectrum of 2-MTP showing several vibronic transitions, including the S_1-S_0 origin band taken at a pulse energy of 400 μJ. The inset depicts schematics of three levels and the chemical structure of 2-MTP. (b) Experimental (black solid) and theoretical (red dotted) R2PI spectra of the S_1-S_0 origin transition of 2-MTP at different pulse energies ranging from 15 to 2500 μJ/pulse. The simulation parameters are provided in Table S1 and Figure S2 in the Supporting Information. Briefly, Γ = 44 ps, μ = 1.42 D, γ = 0.4 cm^{-1}, and $\sigma = 10^{-17}$ cm^2. The laser pulse was not focused. The diameter of the pulse profile is estimated to be 2 mm, and the power density is calculated to be 10^7 W/cm^2 when the laser pulse intensity is 500 μJ/pulse. (c) Peak splitting vs the square root of the laser pulse energy ($I^{1/2}$), giving the straight line with R^2 = 0.992.

multiphoton background signal.[37] Surprisingly, however, the S_1-S_0 origin band that involves the optical transition between the zero-point levels of those two states is found to show clear-cut doublet features as the pump laser intensity increases. The band shape is broadened, and the split of the doublet is linearly proportional to the electric field of the laser light (Figure 1). More interestingly, AT splitting is found to be evident only for the S_1-S_0 origin band. The next three upper-lying R2PI bands above the origin do not show the doublet features even at the strong laser intensity where clear AT splitting for the origin band is observed (Figure 1a), although a tiny AT splitting is observed only in the 103 cm^{-1} vibronic mode (see the Supporting Information). This experimental fact already tells us that the coherent Rabi oscillation is essential for AT splitting even in polyatomic molecules. Namely, for the vibronic transition between states S_1 ($\nu_n' = 1$) and S_0 ($\nu_n'' = 0$), the resonant energy will be $E_1 = E_0 + h\nu_n'$ when quantum numbers for all other vibrational modes except the nth mode are zero. Here, E_0 is the resonant energy for the S_1-S_0 origin band and $h\nu_n'$ is the vibrational energy of the nth mode in state S_1. In this circumstance, the optical field given for the S_1 ($\nu_n' = 1$)$-S_0$ ($\nu_n'' = 0$) transition is not resonant with the most probable transition between states S_1 ($\nu_n' = 1$) and S_0 ($\nu_n'' = 1$) according to the Franck–Condon principle. This would hamper the coherent Rabi oscillation. Naturally, intrusion of multiple states other than the optically coupled states happens quite often in polyatomic molecules, and this is regarded as the intrinsic reason why the laser manipulation of molecules is extremely difficult. Ironically, the experimental fact that only the S_1-S_0 origin band shows the clear-cut doublet feature at the strong optical field once again confirms that our observation originates from AT splitting.

For the interpretation of the experiment, we use the semiclassical optical Bloch equations based on the three-state atomic level model. In this case, the first ($|S_0\rangle$) and second ($|S_1\rangle$) lowest states are optically coupled whereas the third state ($|D_0\rangle$) of the ionized continuum acts as a spectator as depicted in the inset of Figure 1a. The dynamics of three levels could be then described by the following equations.[38]

$$\dot{q} = -\Gamma q - \Omega(t)v - R_{ion}q \tag{1}$$

$$\dot{p} = \Gamma_a q + \Omega(t)v \tag{2}$$

$$\dot{u} = -\gamma_t u - \delta v \tag{3}$$

$$\dot{v} = -\gamma_t v + \delta u + \frac{\Omega(t)}{2}(q - p) \tag{4}$$

q and p are the populations of states S_1 and S_0, respectively. $u(v)$ is the real (imaginary) part of the optical coherence between states S_1 and S_0. Γ is the total decay rate of state S_1. Γ_a is the population decay rate from state S_1 to optically coupled state S_0. It should be noted that we deal with the open system where $\Gamma \gg \Gamma_a$.[33,39] γ_t is the transverse decay rate of the optical coherence given by the relationship $\gamma_t = (\Gamma + \gamma_{laser})/2$, where γ_{laser} is the line width of the pump laser pulse. δ is the frequency detuning from the resonance. The Rabi frequency is given by the equation $\Omega(t) = \Omega_1 \exp[-2(\log 2)t^2/t_0^2]$, where t_0 is the temporal full width at half-maximum (fwhm) of the laser pulse and Ω_1 is the amplitude of the Rabi frequency. The final term on the right-hand side in eq 1 represents the photoionization by the probe photon with a rate $R_{ion}(t) = \lambda\sigma_{ion}I(t)/(hc)$, where σ_{ion} is the photoionization cross section, $I(t) = I_0 \exp[-4(\log 2)t^2/t_0^2]$, and I_0 is the amplitude of the intensity of the ionization laser pulse. As the pump and probe occur with the same laser pulse in our experiment, the relationship $I_0 = \varepsilon_0 c\hbar^2\Omega_1^2/(2\mu^2)$ holds when μ is the transition dipole moment between states S_1 and S_0. The R2PI signal is then given by

$$\int_{-\infty}^{\infty} R_{ion}(t)q(t)\,dt \tag{5}$$

The lifetime (Γ^{-1}) of state S_1 of 2-MTP at its zero-point level has been estimated to be 44 ps.[39] On the basis of empirical parameters, the final band shapes are calculated from eq 5 and then followed by the convolution with a Gaussian function (fwhm of 0.5 cm^{-1}) (see the Supporting Information). Remarkably, the simulation by the numerical solution reproduces the experiment extremely well (Figure 1b). The AT splitting behavior in terms of the increase in the split with an increase in the square root of the laser intensity and the peak broadening are nicely reproduced by the simulation.

We employ the dressed-state approach to gain further physical insights. Here, the population of state S_1 (q) is given as follows[40]

$$q = p_1 \sin^2\theta + p_2 \cos^2\theta \tag{6}$$

https://dx.doi.org/10.1021/acs.jpclett.0c01918
J. Phys. Chem. Lett. 2020, 11, 6791−6795

$$\sin^2\theta = \frac{1}{2}\left(1 + \frac{\delta}{\sqrt{\delta^2 + \Omega_1^{\,2}}}\right) \tag{7}$$

$$\cos^2\theta = \frac{1}{2}\left(1 - \frac{\delta}{\sqrt{\delta^2 + \Omega_1^{\,2}}}\right) \tag{8}$$

where p_1 and p_2 are the populations of the low and upper dressed states, respectively. On the right-hand side of eq 6, the off-diagonal density matrix element, $-\sin 2\theta\ \mathrm{Re}(\rho)$, has been ignored as it is very weak under our experimental condition, where ρ is the optical coherence in the dressed state. As both dressed states of p_1 and p_2 are strongly coupled, the density matrix equations could be numerically solved to give the effective excited-state population as a function of the detuning frequency (δ) (see the Supporting Information) (Figure 2). In

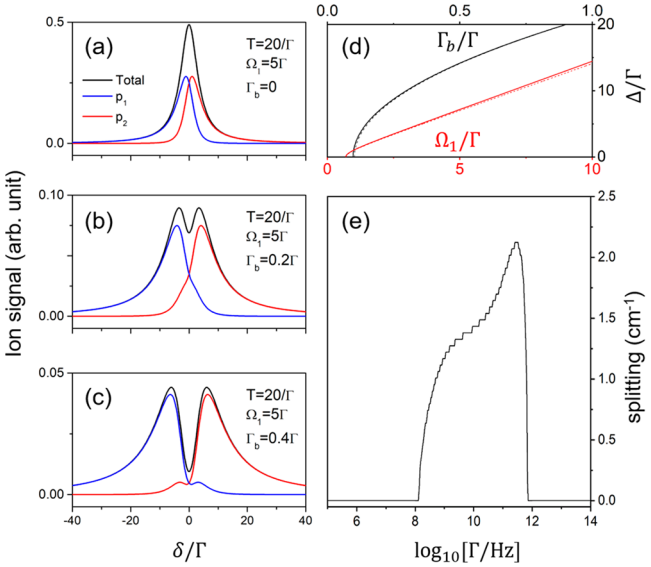

Figure 2. Calculated excited-state populations decomposed into the distinct contributions of p_1 (blue) and p_2 (red) dressed states as a function of the detuning frequency when (a) $\Gamma_b = 0$, (b) $\Gamma_b = 0.2\Gamma$, or (c) $\Gamma_b = 0.4\Gamma$. (d) Behavior of Δ as a function of Γ_b (black) and Ω_1 (red). For the plot of Δ vs Γ_b, parameters were set to be $T = 20/\Gamma$, $\gamma_t = 0.5\Gamma$, and $\Omega_1 = 5\Gamma$. For the Ω_1 dependence of Δ, the following parameters were used: $T = 20/\Gamma$, $\gamma_t = 0.5\Gamma$, and $\Gamma_b = 0.2\Gamma$. In both cases, numerical (solid) and analytic solutions from eq 10 (dashed) agree very well. (e) Calculated splitting as a function of log Γ from eq 11; all of the parameters are the same as those of 2-MTP at 500 μJ/pulse. As the detuning varies from zero, the effective Rabi frequency increases and the energy level of each eigenstate shifts. When the laser frequency is scanned, each contribution smears out and becomes broad, and thus, the centers of the accumulated populations of two dressed states are located at the non-zero detuning.

either case, the analytic solution is obtained under the assumption $\Gamma_b \equiv \Gamma - \Gamma_a \ll \Gamma$, where Γ_b is the rate of decay of state S_1 into states other than the ground state. This assumption of $\Gamma_b \ll \Gamma$ was necessary for the analytical solution to the rate equations of eqs 1−4, which sounds quite contradictory to the experimental condition of $\Gamma \gg \Gamma_a$. However, the resultant analytical solution is surprisingly found to be quite consistent with the accurate numerical solution, as shown Figure 2d as follows. The resultant analytic form of q is then given by

$$q = \frac{\gamma_t\Omega_1^{\,2}/2}{\Gamma(\delta^2 + \gamma_t^{\,2}) + \gamma_t\Omega_1^{\,2}} \exp\left[-\frac{\Gamma_b\gamma_t\Omega_1^{\,2}T/2}{\Gamma(\delta^2 + \gamma_t^{\,2}) + \gamma_t\Omega_1^{\,2}}\right] \tag{9}$$

where T is defined as the time window for the ionization detection. The maxima of q are obtained by differentiating eq 9 with respect to δ, and the separation (Δ) of the doublet is given by

$$\Delta = \sqrt{2\gamma_t\left(\frac{\Gamma_b T - 2}{\Gamma}\Omega_1^{\,2} - 2\gamma_t\right)} \tag{10}$$

The splitting value (Δ) calculated from the dressed-atom approach as a function of Γ_b and Ω_1 is shown in Figure 2d. Although eq 10 is valid only if $\Gamma_b \ll \Gamma$, it is still fully consistent with the result from the numerical solution for a wide range of Γ_b values. It is evident that two dressed states of p_1 and p_2 merge into a singlet when $\Gamma_b = 0$, indicating that discrimination of two dressed states is not anticipated for the closed system. As the system becomes opened giving a Γ_b of 0.2Γ or 0.4Γ, two dressed states split to give a clear doublet feature (Figure 2a−c). Intuitively, when the system is closed, the population of state S_1 at the resonance is expected to be larger than that at the off-resonant detuning. As the system becomes more opened, the population of state S_1 at the resonance is depleted more substantially than that at the off-resonant detuning. This makes the off-resonant populations of dressed states at detuned frequencies stand out, giving the apparent AT splitting.

Interestingly, we could extract the threshold condition for the observation of the non-zero AT split value as follows.

$$\Gamma_b T \geq 2\left(1 + \frac{\Gamma\gamma_t}{\Omega_1^{\,2}}\right) \tag{11}$$

For 2-MTP, the S−H predissociation is the major dephasing process of state S_1 that satisfies the open-system condition of $\Gamma_b \approx \Gamma$,[33,39] rationalizing the AT splitting observation even at the low laser intensity. In these circumstances, Δ is proportional to $\sqrt{\gamma_t}$, suggesting that AT splitting strongly depends on the excited-state lifetime ($\tau = 1/\Gamma$). Namely, as the state S_1 lifetime decreases, the AT split energy gap increases. If the laser intensity is 500 μJ/pulse, AT splitting is predicted to be observed when τ is smaller than hundreds of picoseconds (Figure 2e).

To verify our theoretical analysis of AT splitting, we have carried out similar experiments on 2-fluorothiophenol (2-FTP) and 2-chlorothiophenol (2-CTP); their state S_1 lifetimes have been measured to be 12.3 and 227 ps, respectively.[39] Remarkably, for both 2-FTP and 2-CTP, AT splitting is observed only for the S_1−S_0 origin band, and its behavior with the laser intensity exactly follows the theoretical prediction (Figure 3). The plot of AT splitting versus the square root of the laser intensity for all three molecules (2-MTP, 2-FTP, and 2-CTP) shows a straight line. AT splitting of 2-FTP especially stands out giving the largest Δ, whereas that of 2-CTP shows a much reduced AT split value. This is quite consistent with our model. It should be noted that Δ depends on both Γand μ. The transition dipole moment calculated from the EOM-CCSD method gives μ values of 0.94, 1.42, and 0.60 D for 2-FTP, 2-MTP, and 2-CTP, respectively.[32,41] Although these values do not predict the experiment quantitatively, the qualitative trend among these three cases could be partially

https://dx.doi.org/10.1021/acs.jpclett.0c01918
J. Phys. Chem. Lett. 2020, 11, 6791−6795

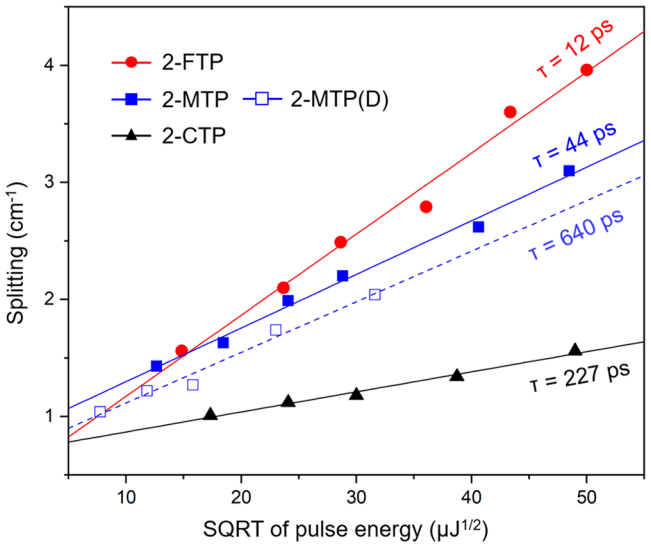

Figure 3. Experimental AT splitting vs the square root of the pulse energy for 2-FTP (red circles), 2-MTP (blue filled squares), 2-MTP(D) (blue empty squares), and 2-CTP (black triangles). Lines are the least-squares fits to the experiments. In principle, the slope of the data should follow eq 10, yet it should be noted that eq 10 behaves approximately linearly with Ω_1 only when the Rabi frequency is sufficiently large. The typical graph from eq 10 will decrease to the zero at small values of Ω_1. The offset on the *y*-axis could be due to the fitting error and/or the intrinsic property of eq 10.

explained. It should be noted that AT splitting of 2-MTP(D) of which the SH moiety is substituted by SD is less pronounced compared to that of 2-MTP, yet it stands out compared to that of 2-CTP. As the lifetime of 2-MTP(D) is estimated to be 640 ps,[39] AT splitting of 2-MTP(D) is supposed to be much less pronounced compared to that of 2-CTP (τ = 227 ps). This inconsistency should come from our simplified three-state atomic model employed in treating the complex molecular systems. As the molecule becomes more complicated, the atomic model is less validated in general. For instance, 2-MTP is the even more complex system compared to 2-FTP or 2-CTP as the number of degrees of freedom ($3N - 6$) is 45 for 2-MTP but only 33 for 2-FTP and 2-CTP. The influence of the complexity on the state dressing of polyatomic molecular system should definitely be examined further in the near future.

In summary, Autler–Townes splitting, which has long been considered to be negligible in polyatomic molecules, has been experimentally observed here for the first time in the optical transition between the zero-point levels of states S_1 and S_0 of polyatomic molecules of 2-methoxythiophenol, 2-fluorothiophenol, and 2-chlorothiophenol. It has been found, through the semiclassical optical Bloch equations and dressed-atom approach based on the three-level atomic model, that the optical dressing of quantum states is plausible even for the polyatomic molecule if it provides the open system of which the excited-state lifetime is shorter than hundreds of picoseconds. The AT splitting observed here in large molecules sheds new light on the optical manipulation of polyatomic molecular system in a variety of ways.

EXPERIMENTAL METHODS

The details of the experimental setup had been reported elsewhere.[30] Briefly, the samples were heated to 30–100 °C in the reservoir to achieve the proper vapor pressure, mixed with helium or neon, and expanded through a nozzle orifice (Even-Lavie valve) into a high-vacuum chamber with a backing pressure of 2–10 atm at 10 Hz. The resultant supersonic jet was collimated by a 1 mm diameter skimmer before it was crossed by the nanosecond ultraviolet (UV) laser pulse that was obtained by frequency doubling of the dye laser (Lumonics HD-500) pumped by the second harmonic of a Nd:YAG laser (Surelite II-10). The ion signal was detected by a mass-gated time-of-flight multichannel plate (MCP) detector, digitized by an oscilloscope, and stored in the computer. The signal was averaged for 160 laser shots while the scanning interval was fixed at 0.002 nm for each measurement. The intensity of the UV laser pulse was finely tuned by the combination of several reflective neutral density filters in the range of 10–3000 μJ/pulse.

ASSOCIATED CONTENT

Supporting Information

The Supporting Information is available free of charge at https://pubs.acs.org/doi/10.1021/acs.jpclett.0c01918.

Details in the derivation of equations in the main text, dressed analysis for an open two-level atomic system, parameters and Rabi frequency used in the simulation, AT splitting in other vibronic bands, PGOPHER simulation of the REMPI spectrum of 2MTP, R2PI spectra of the S_1–S_0 origin band of 2-FTP and 2-CTP, and two-color R2PI spectrum of 2-MTP (PDF)

AUTHOR INFORMATION

Corresponding Authors

Heung-Ryoul Noh – *Department of Physics, Chonnam National University, Gwangju 61186, Republic of Korea*; Email: hrnoh@chonnam.ac.kr

Sang Kyu Kim – *Department of Chemistry, KAIST, Daejeon 34141, Republic of Korea*; orcid.org/0000-0003-4803-1327; Email: sangkyukim@kaist.ac.kr

Authors

Junggil Kim – *Department of Chemistry, KAIST, Daejeon 34141, Republic of Korea*

Jean Sun Lim – *Department of Chemistry, KAIST, Daejeon 34141, Republic of Korea*

Complete contact information is available at: https://pubs.acs.org/10.1021/acs.jpclett.0c01918

Notes

The authors declare no competing financial interest.

ACKNOWLEDGMENTS

This work has been supported by the National Research Foundation of Korea (NRF) under Projects 2019R1A6A1A10073887, 2018R1A2B3004534 (S.K.K.), and 2020R1A2C1005499 (H.-R.N.).

REFERENCES

(1) Autler, S. H.; Townes, C. H. Stark Effect in Rapidly Varying Fields. *Phys. Rev.* **1955**, *100*, 703.

(2) Aspect, A.; Arimondo, E.; Kaiser, R.; Vansteenkiste, N.; Cohen-Tannoudji, C. Laser Cooling Below the One-Photon Recoil Energy by Velocity-Selective Coherent Population Trapping. *Phys. Rev. Lett.* **1988**, *61*, 826.

(3) Morigi, G.; Eschner, J.; Keitel, C. H. Ground State Laser Cooling Using Electromagnetically Induced Transparency. *Phys. Rev. Lett.* **2000**, *85*, 4458.
(4) Gray, H. R.; Whitley, R. M.; Stroud, C. R., Jr. Coherent Trapping of Atomic Populations. *Opt. Lett.* **1978**, *3*, 218.
(5) Sussman, B. J.; Townsend, D.; Ivanov, M. Y.; Stolow, A. Dynamic Stark Control of Photochemical Processes. *Science* **2006**, *314*, 278.
(6) Sanz-Sanz, C.; Richings, G. W.; Worth, G. A. Dynamic Stark Control: Model Studies Based on the Photodissociation of IBr. *Faraday Discuss.* **2011**, *153*, 275.
(7) Sola, I. R.; Gonzalez-Vazquez, J.; de Nalda, R.; Banares, L. Strong Field Laser Control of Photochemistry. *Phys. Chem. Chem. Phys.* **2015**, *17*, 13183.
(8) Liao, P. F.; Bjorkholm, J. E. Direct Observation of Atomic Energy Level Shifts in Two-Photon Absorption. *Phys. Rev. Lett.* **1975**, *34*, 1540.
(9) Cahuzac, Ph.; Vetter, R. Observation of the Autler-Townes Effect on Infrared Laser Transitions of Xenon. *Phys. Rev. A: At., Mol., Opt. Phys.* **1976**, *14*, 270.
(10) Delsart, C.; Keller, J. − C. Observation of the Optical Autler-Townes Splitting in Neon Gas with a Cascade Level Scheme. *J. Phys. B: At. Mol. Phys.* **1976**, *9*, 2769.
(11) Gray, H. R.; Stroud, C. R., Jr. Autler-Townes Effect in Double Optical Resonance. *Opt. Commun.* **1978**, *25*, 359.
(12) Fort, C.; Cataliotti, F. S.; Raspollini, P.; Tino, G. M.; Inguscio, M. Optical Double-Resonance Spectroscopy of Trapped Cs Atoms: Hyperfine Structure of the 8s and 6d Excited States. *Z. Phys. D: At., Mol. Clusters* **1995**, *34*, 91.
(13) Xu, X.; Sun, B.; Berman, P. R.; Steel, D. G.; Bracker, A. S.; Gammon, D.; Sham, L. J. Coherent Optical Spectroscopy of a Strongly Driven Quantum Dot. *Science* **2007**, *317*, 929.
(14) Wagner, M.; Schneider, H.; Stehr, D.; Winnerl, S.; Andrews, A. M.; Schartner, S.; Strasser, G.; Helm, M. Observation of the Intraexciton Autler-Townes Effect in GaAs/AlGaAs Semiconductor Quantum Wells. *Phys. Rev. Lett.* **2010**, *105*, 167401.
(15) Novikov, S.; Sweeney, T.; Robinson, J. E.; Premaratne, S. P.; Suri, B.; Wellstood, F. C.; Palmer, B. S. Raman Coherence in a Circuit Quantum Electrodynamics Lambda System. *Nat. Phys.* **2016**, *12*, 75.
(16) Qi, J.; Lazarov, G.; Wang, X.; Li, L.; Narducci, L. M.; Lyyra, A. M.; Spano, F. C. Autler-Townes Splitting in Molecular Lithium: Prospects for All-Optical Alignment of Nonpolar Molecules. *Phys. Rev. Lett.* **1999**, *83*, 288.
(17) Schlöder, U.; Deuschle, T.; Silber, C.; Zimmermann, C. Autler-Townes Splitting in Two-Color Photoassociation of ^{6}Li. *Phys. Rev. A: At., Mol., Opt. Phys.* **2003**, *68*, 051403.
(18) Sun, Z.; Lou, N. Autler-Townes Splitting in the Multiphoton Resonance Ionization Spectrum of Molecules Produced by Ultrashort Laser Pulses. *Phys. Rev. Lett.* **2003**, *91*, 023002.
(19) Garcia-Fernandez, R.; Ekers, A.; Klavins, J.; Yatsenko, L. P.; Bezuglov, N. N.; Shore, B. W.; Bergmann, K. Autler-Townes Effect in a Sodium Molecular-Ladder Scheme. *Phys. Rev. A: At., Mol., Opt. Phys.* **2005**, *71*, 023401.
(20) Otis, C. E.; Johnson, P. M. The AC Stark Effect in Molecular Multiphoton Ionization Spectroscopy. *Chem. Phys. Lett.* **1981**, *83*, 73.
(21) Girard, B.; Billy, N.; Vigue, J.; Lehmann, J. C. Evidence for a Dynamical Stark Effect in CO($A^1\Pi$) Two-Photon Excitation. *Chem. Phys. Lett.* **1983**, *102*, 168.
(22) Huo, W. M.; Gross, K. P.; McKenzie, R. L. Optical Stark Effect in the Two-Photon Spectrum of NO. *Phys. Rev. Lett.* **1985**, *54*, 1012.
(23) Quesada, M. A.; Lau, A. M. F.; Parker, D. H.; Chandler, D. W. Observation of Autler-Townes Splitting in the Multiphoton Ionization of H_2: Measurement of Vibronic Transition Moments Between Excited Electronic States. *Phys. Rev. A: At., Mol., Opt. Phys.* **1987**, *36*, 4107.
(24) Xu, S.; Sha, G.; Jiang, B.; Sun, W.; Chen, X.; Zhang, C. Two-Color Study of Autler-Townes Doublet Splitting and AC Stark Shift in Multiphoton Ionization Spectra of CO. *J. Chem. Phys.* **1994**, *100*, 6122.
(25) Lee, C. Y.; Pate, B. H. Dressed States of Molecules and Microwave-Infrared Double-Resonance Spectroscopic Techniques Employing an Electric Quadrupole Focusing Field. *J. Chem. Phys.* **1997**, *107*, 10430.
(26) Kim, Y.; Hall, G. E.; Sears, T. J. AC Stark Detection of Optical-Optical Double Resonance in CH_2. *Phys. Chem. Chem. Phys.* **2006**, *8*, 2823.
(27) Duxbury, G.; Kelly, J. F.; Blake, T. A.; Langford, N. The AC Stark Effect in Nitric Oxide Induced by Rapidly Swept Continuous Wave Quantum Cascade Lasers. *J. Chem. Phys.* **2012**, *136*, 174318.
(28) Schmitz, D.; Shubert, V. A.; Patterson, D.; Krin, A.; Schnell, M. Phase Dependence of Double-Resonance Experiments in Rotational Spectroscopy. *J. Phys. Chem. Lett.* **2015**, *6*, 1493.
(29) Roenitz, K. M.; Hays, B. M.; Powers, C. R.; McCabe, M. N.; Smith, H.; Widicus Weaver, S. L.; Shipman, S. T. AC Stark Effect Observed in a Microwave-Millimeter/Submillimeter Wave Double-Resonance Experiment. *J. Phys. Chem. A* **2018**, *122*, 6321.
(30) Lim, J. S.; Kim, S. K. Experimental Probing of Conical Intersection Dynamics in the Photodissociation of Thioanisole. *Nat. Chem.* **2010**, *2*, 627.
(31) Lee, J.; Kim, S. − Y.; Kim, S. K. Spectroscopic Study on Nonradiative Transition and Ionization of 5-methylpyrimidine at S_1 Probed by the Slow-Electron Velocity-Map Imaging (SEVI) Technique. *Chem. Phys. Lett.* **2013**, *568*−*569*, 36.
(32) Han, S.; You, H. S.; Kim, S. − Y.; Kim, S. K. Dynamic Role of the Intramolecular Hydrogen Bonding in Nonadiabatic Chemistry Revealed in the UV Photodissociation Reactions of 2-Fluorothiophenol and 2-Chlorothiophenol. *J. Phys. Chem. A* **2014**, *118*, 6940.
(33) Lim, J. S.; You, H. S.; Kim, S. − Y.; Kim, J.; Park, Y. C.; Kim, S. K. Vibronic Structure and Predissociation Dynamics of 2-Methoxythiophenol (S_1): The Effect of Intramolecular Hydrogen Bonding on Nonadiabatic Dynamics. *J. Chem. Phys.* **2019**, *151*, 244305.
(34) Gerhards, M.; Perl, W.; Kleinermanns, K. Rotamers and Vibrations of Resorcinol Obtained by Spectral Hole Burning. *Chem. Phys. Lett.* **1995**, *240*, 506.
(35) Dean, J. C.; Navotnaya, P.; Parobek, A. P.; Clayton, R. M.; Zwier, T. S. Ultraviolet Spectroscopy of Fundamental Lignin Subunits: Guaiacol, 4-Methylguaiacol, Syringol, and 4-Methylsyringol. *J. Chem. Phys.* **2013**, *139*, 144313.
(36) Western, C. M.; Billinghurst, B. E. Automatic Assignment and Fitting of Spectra with PGOPHER. *Phys. Chem. Chem. Phys.* **2017**, *19*, 10222.
(37) Shimoda, K. *High-Resolution Laser Spectroscopy*; Springer-Verlag: Berlin, 1976.
(38) Porfido, N.; Bezuglov, N. N.; Bruvelis, M.; Shayeganrad, G.; Birindelli, S.; Tantussi, F.; Guerri, I.; Viteau, M.; Fioretti, A.; Ciampini, D.; Allegrini, M.; Comparat, D.; Arimondo, E.; Ekers, A.; Fuso, F. Nonlinear Effects in Optical Pumping of a Cold and Slow Atomic Beam. *Phys. Rev. A: At., Mol., Opt. Phys.* **2015**, *92*, 043408.
(39) Woo, K. C. State- and Time-Resolved Excited-State Photodissociation Dynamics beyond the Born-Oppenheimer Approximation. Ph.D. Thesis, Korea Advanced Institute of Science and Technology, Daejeon, Korea, 2019.
(40) Berman, P. R.; Malinovsky, V. S. *Principles of laser spectroscopy and quantum optics*; Princeton University Press: Princeton, NJ, 2011.
(41) Lim, J. S.; You, H. S.; Han, S.; Kim, S. K. Photodissociation Dynamics of Ortho-Substituted Thiophenols at 243 nm. *J. Phys. Chem. A* **2019**, *123*, 2634.

https://dx.doi.org/10.1021/acs.jpclett.0c01918
J. Phys. Chem. Lett. 2020, 11, 6791−6795